

# Supporting Information

## Molecular Mechanism of Avibactam Mediated $\beta$ -Lactamase Inhibition

Dustin T. King<sup>‡,1</sup>, Andrew M. King<sup>‡,2</sup>, Sarah M. Lal<sup>2</sup>, Gerard D. Wright<sup>‡,2</sup>, Natalie C.J. Strynadka<sup>\*,1</sup>

<sup>‡</sup>These authors contributed equally

<sup>1</sup>The Department of Biochemistry and Molecular Biology and Center for Blood Research, University of British Columbia. 2350 Health Sciences Mall, Vancouver, British Columbia, V6T 1Z3, Canada

<sup>2</sup>M.G. Department of Biochemistry and Biomedical Sciences and the Department of Chemistry, DeGroote Institute for Infectious Disease Research, McMaster University, Hamilton, Ontario, L8S 4K1, Canada

### TABLE OF CONTENTS

Methods.....	S2
Dynamic light scattering.....	S2
LC-MS analysis of avibactam-CTX-M-15 mutants.....	S2
Protein expression and purification for crystallographic studies.....	S2
Tables.....	S3
Table S1. Data collection and refinement statistics.....	S3
Table S2. Primers used in this study. Underline shows restriction sites.....	S4
Table S3. Kinetic values for the hydrolysis of nitrocefin by CTX-M-15 mutants.....	S5
Figures.....	S6
Figure S1. Carbamyl-avibactam bound CTX-M-15 active site details.....	S6
Figure S2. Avibactam electron density for carbamylated CTX-M-15, OXA-48 and OXA-10.....	S7
Figure S3. CTX-M-15 variants are stable in solution.....	S8
Figure S4. Interactions between avibactam and active site residues in OXA-48 and OXA-10.....	S9
Figure S5. Carboxylation of the SXXK lysine in OXA-48 and OXA-10.....	S10
Figure S6. Comparison of carbamyl-avibactam CTX-M-15, OXA-48 and AmpC co-crystal structures.....	S11
Figures 7-16. ESI-LC-MS trace overlays of avibactam incubated with $\beta$ -lactamase at pH 7.5.....	S12-S21
References.....	S22

## METHODS

### Dynamic light scattering.

Dynamic light scattering was performed using a Zetasizer NanoS (Malvern Instruments). All measurements were taken using a 12  $\mu$ L quartz cell (ZEN2112) at 25°C. Size distribution of the samples was calculated based on the correlation function provided by the Zetasizer Nano S software.

### LC-MS analysis of avibactam-CTX-M-15 mutants.

LC-ESI-MS data were obtained by using an Agilent 1100 Series LC system (Agilent Technologies Canada, Inc.) and a QTRAP LC/MS/MS System (Applied Biosystems). The reverse phase HPLC was performed using C<sub>18</sub> column (SunFire C18 5  $\mu$ m, 4.6x50 mm, Waters) with Agilent 1100 LC binary pump at a flow rate of 1 mL/min, under the following conditions: isocratic 5% solvent B (0.05% formic acid in acetonitrile) and 95% solvent A (0.05% formic acid in water) for 1 min, followed by a linear gradient to 97% B over 10 min. CTX-M-15 WT, K73A, N104A, S130A, N132A, E166Q, K234A; and KPC-2 (7  $\mu$ M) were incubated with 14  $\mu$ M avibactam in buffer containing 30 mM HEPES pH 7.5, 300 mM NaCl, and 20 % v/v glycerol and analyzed at both 0 h and 24 h.





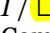







### Protein expression and purification for crystallographic studies.

The *P. aeruginosa* OXA-10 protein (UniProt ID: P14489) corresponding to the mature sequence (20-266) was cloned, overexpressed and purified as previously described<sup>1</sup>.

The *E. coli* CTX-M-15 and *Klebsiella pneumoniae* OXA-48 expression vectors were constructed as described above. The expression vectors were then transformed into *E. coli* BL21 DE3 cells. The cells were grown in Lauria Bertani (LB) broth at 37°C until an OD<sub>600</sub> of 0.7 was reached at which point the culture was cooled to room temperature. Protein expression was induced by addition of 1mM isopropyl  $\beta$ -D-1-thiogalactopyranoside (IPTG) and the cultures were grown at 22°C for 12-16 hours. The cells (~20g) were then harvested and resuspended in 50mL lysis buffer (50mM Tris, pH 7.5, 350mM NaCl, and one complete, EDTA-free protease inhibitor tablet from Roche). The cells were lysed by two passes on a French Press at ~12,000 p.s.i., and the lysate was centrifuged (45,000 rpm in a Beckman 70 Ti rotor) for 35 minutes. The supernatant was then filtered using a 0.22  $\mu$ m syringe filter and passed through a 1mL Hi-Trap HP His column, which was pre-equilibrated in lysis buffer. Elution buffer (50 mM Tris, pH 7.5, 350mM NaCl, 1M imidazole) was used to elute the His-tagged proteins from the column with a gradient of imidazole from 0 to 500mM in 50 minutes. Fractions enriched in the protein of interest were pooled and 1U/mL of bovine  $\alpha$ -thrombin (Roche) was added and the samples were incubated overnight at 4°C. Samples were then exchanged via a 10 kDa cut-off Amicon centrifugation concentrator into crystallization buffer (20mM Tris, pH 7.5, 100mM NaCl). Samples were passed over a Superdex 200 column using crystallization buffer, as running buffer and pooled fractions were concentrated to 30 mg/mL for CTX-M-15, 50 mg/mL for OXA-48 and 10mg/mL for OXA-10.

## TABLES

Table S1. Data collection and refinement statistics.

	CTX-M-15- AVI	OXA-10-AVI	OXA-48- AVI8.5	OXA-48- AVI7.5	OXA-48- AVI6.5	OXA-48- Native
<b>Data collection</b>						
Space group	P <sub>2</sub> <sub>1</sub>	P <sub>2</sub> <sub>1</sub> 2 <sub>1</sub> 2 <sub>1</sub>	P <sub>3</sub> <sub>2</sub>	P <sub>3</sub> <sub>2</sub>	P <sub>2</sub> <sub>1</sub> 2 <sub>1</sub> 2 <sub>1</sub>	P <sub>2</sub> <sub>2</sub> 2 <sub>1</sub> 2 <sub>1</sub>
Cell dimensions  a, b, c (Å)	62.0, 60.6, 71.5	48.6, 96.5, 125.7	142.0, 142.0, 52.4	142.8, 142.8, 52.4	64.1, 108.1, 162.8	43.4, 102.9, 124.7
  (°)	90, 104, 90	90, 90, 90	90, 90, 120	90, 90, 120	90, 90, 90	90, 90, 90
Resolution (Å)	34.7-1.6 (1.69- 1.60)	52.66-1.70 (1.73-1.70)	46.64-2.00 (2.11-2.00)	52.42-2.10 (2.21-2.10)	65.03-2.54 (2.65-2.54)	41.6-1.70 (1.73-1.70)
R <sub>merge</sub>  I / 	0.052(0.296) 13.7(3.5)	0.040(0.290) 24.5(5.2)	0.090(0.295) 6.1(2.9)	0.096(0.457) 8.5(2.9)	0.065(0.150) 12.7(6.1)	0.055(0.424) 12.1(2.3)
Completeness (%)	96.7(95.2)	98.0(99.9)	99.2(99.4)	99.8(100.0)	91.2(91.4)	99.7(99.9)
Redundancy	3.9(3.9)	4.8(4.9)	2.5(2.5)	3.4(3.4)	4.0(3.8)	5.0(4.9)
<b>Refinement</b>						
Resolution (Å)	34.7-1.60	52.66-1.70	46.64-2.00	52.42-2.10	65.03-2.54	41.6-1.70
No. reflections	65645(9368)	64493(3478)	76256(11167)	69650(10200)	34471(4158)	62226(3297)
R <sub>work</sub> / R <sub>free</sub>	0.165/0.198	0.185/0.230	0.171%/0.205	0.172/0.205	0.184/0.222	0.192/0.226
Avibactam occupancy chainA, chainB, etc.	1.00, 1.00	1.00, 1.00	0.70, 0.70, 1.00, 1.00	1.00, 1.00, 1.00, 1.00	1.00, 1.00, 1.00, 1.00	N/A, N/A
No. atoms						
Protein	3930	3957	8000	8043	7972	3963
Ligand/ion	34	38	68	68	68	N/A
Water	549 	468 	362 	480 	203 	372 
B-factors 						
Protein	17.8	22.6	40.2	30.3	34.1	27.2
Ligand/ion	17.8	17.5	36.7	22.4	35.4	N/A
Water	27.4	28.7	37.6	32.3	29.2	35.4
R.m.s. deviations						
Bond lengths (Å)	0.012	0.012	0.014	0.012	0.011	0.014
Bond angles (°)	1.62	1.70	1.72	1.68	1.49	1.53
Favored/allowed/ disallowed (%) <sup>+</sup>	98.2, 1.4, 0.4	97.8, 2.0, 0.2	97.6, 2.4, 0.0	97.2, 2.8, 0.0	97.9, 2.1, 0.0	97.7, 2.3, 0.0

\*All datasets correspond to diffraction data collected from a single crystal.

\*Values in parentheses are for highest-resolution shell.

\*Avibactam (AVI)

<sup>+</sup>phenix.ramalyze; “allowed” is the percentage remaining after “favored” and “outlier” residues are subtracted.

Table S2. Primers used in this study. Underline shows restriction sites.

Primer	Sequence (5'-3')
CTX-M-15 F	AATATCATATGCAAACGGCGGACGTACAGCA
CTX-M-15 R	TATTAGAATTCTTACCGTCGGTGACGATTTTAGCC
OXA-48 F	GCTTCATATGGAATGGCAAGAAAACAAAAGTTGGAATGCT
OXA-48 R	CGTACTCGAGCTAGGGAATAATTTTTTTCCTGTTTGAGCAC
K73A F	GCGATGTGCAGCACCAGTGCGGTGATGG
K73A R	CGCTACACGTCGTGGTCACGCCACTACC
N104A F	CGAGTTGAGATCAAAAAATCTGACCTTGTTGCGTATAATCCGATTGC
N104A R	GCTCAACTCTAGTTTTTTTAGACTGGAACAACGCATATTAGGCTAACG
S130A F	CGCTACAGTACGCGGATAACGTGGCGATGAATAAGC
S130A R	GCGATGTCATGCGCCTATTGCACCGCTACTTATTTCG
N132A F	GCTACAGTACAGCGATGCGGTGGCGATGAATAAGC
N132A R	CGATGTCATGTCGCTACGCCACCGCTACTTATTTCG
E166Q F	GCTGGGAGACGAAACGTTCCGTCTCGACC
E166Q R	CGACCCTCTGCTTTGCAAGGCAGAGCTGG
K234A F	GGTTGTGGGGGATGCGACCGGCAGC
K234A R	CCAACACCCCCTACGCTGGCCGTCG
T7 terminator	GCTAGTTATTGCTCAGCGG

Table S3. Kinetic values for the hydrolysis of nitrocefin by CTX-M-15 mutants.

<b>Parameter</b>	<b><i>WT</i></b>	<b><i>K73A</i></b>	<b><i>N104A</i></b>	<b><i>S130A</i></b>	<b><i>N132A</i></b>	<b><i>E166Q</i></b>	<b><i>K234A</i></b>
$K_m$ ( $\mu\text{M}$ )	9.9	13	11	33	6.2	8.3	2.6
$k_{\text{cat}}$ ( $\text{s}^{-1}$ )	57	4.1	85	270	55	0.06	4.0
$k_{\text{cat}}/K_m$ ( $\text{M}^{-1} \text{s}^{-1}$ )	$5.8 \times 10^6$	$3.1 \times 10^5$	$8.2 \times 10^6$	$8.2 \times 10^6$	$8.8 \times 10^6$	$7.9 \times 10^3$	$1.6 \times 10^6$

## FIGURES

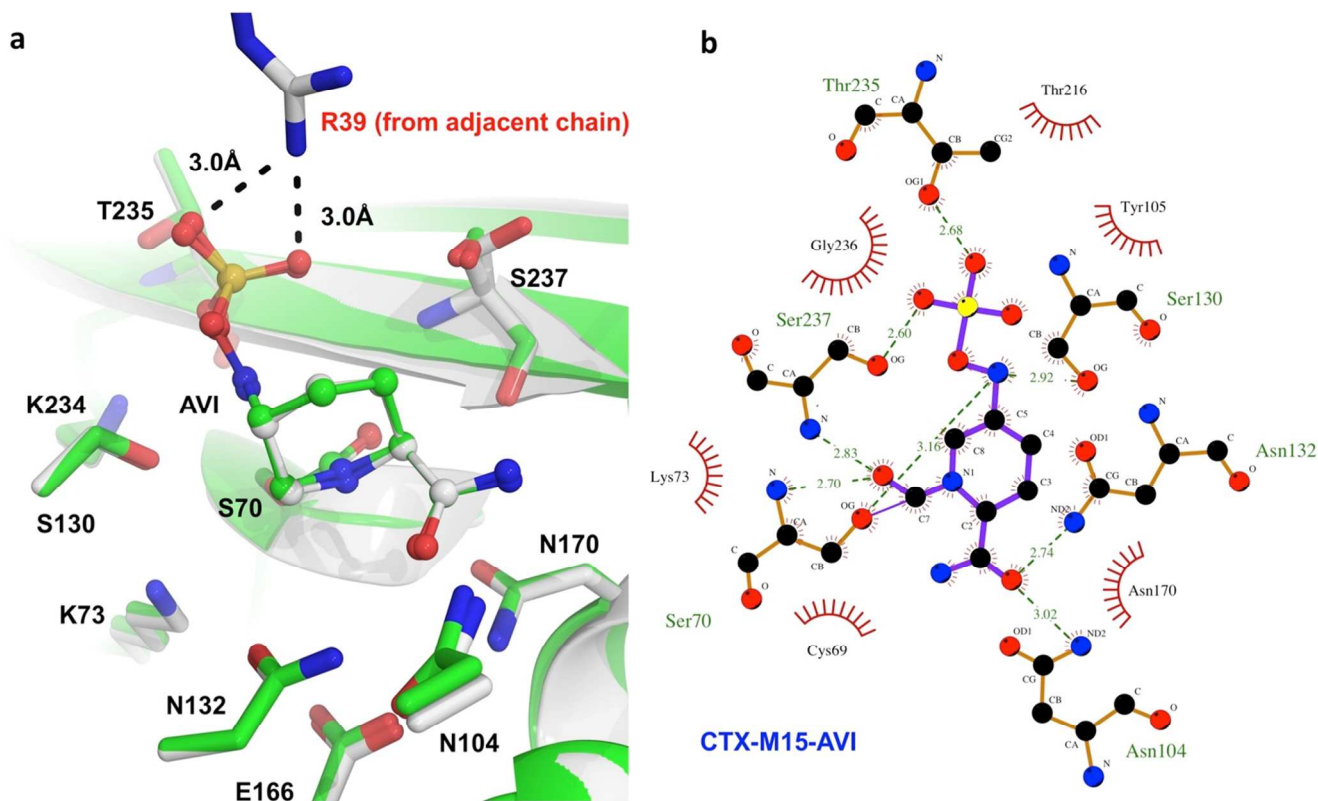


Figure S1. Carbamyl-avibactam bound CTX-M-15 active site details. (a) Active site overlay of carbamyl-avibactam and CTX-M-15 complex in spacegroups  $P2_12_12_1$  (PDB ID: 4HBU)<sup>2</sup>, and  $P2_1$  (PDB ID: XXXX). Carbon atoms for the 4HBU and XXXX active site residues and avibactam are displayed in grey and green, with all other non-carbon atoms colored by type (N, blue; O, red; S, yellow). The 4HBU and XXXX CTX-M-15 protein backbones are displayed as grey and green cartoons. (b) Protein-ligand interactions between CTX-M-15 and avibactam depicted in monomer A using LigPlot<sup>3</sup>. Avibactam and CTX-M-15 are displayed as purple and orange sticks with atoms colored by type. Hydrogen bonding and electrostatic interactions are shown as green dashes. Ligand-protein hydrophobic contacts are shown as curved red combs.

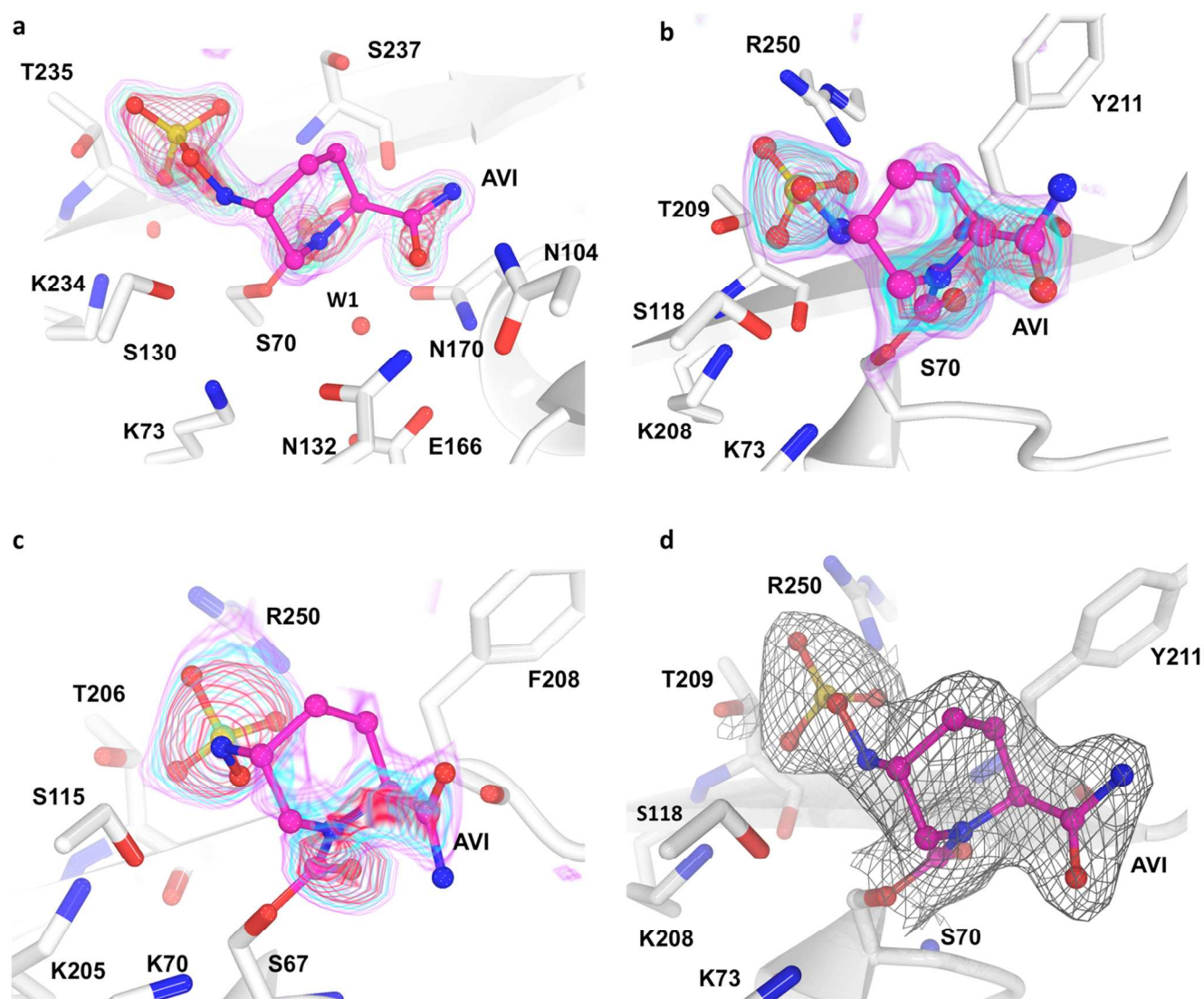


Figure S2. Avibactam electron density for carbamylated CTX-M-15, OXA-48 and OXA-10 crystal structures. In a-c, the  $F_o-F_c$  ligand omit maps are contoured at 3.0, 4.0 and 5.0  $\sigma$  and are shown as pink, cyan and red transparent surfaces. (a) Carbamyl-avibactam CTX-M-15 ligand omit  $F_o-F_c$  electron density. The CTX-M-15 cartoon is shown in white with selected active site residues displayed in stick representation and non-carbon atoms are colored by type. (b) and (c), Carbamyl-avibactam OXA-48-AVI7.5 and OXA-10 ligand omit  $F_o-F_c$  electron density. In B and C, the OXA-48-AVI7.5 and OXA-10 protein backbones are shown in white cartoon representation with selected active site residues displayed as white sticks with non-carbon atoms colored by type. In all panels, the carbamyl-avibactam is represented as pink sticks with atoms colored by type. (d) Carbamyl-avibactam OXA-48-AVI7.5 final refined  $2F_o-F_c$  electron density. The OXA-48-AVI7.5 protein and bound avibactam are displayed as in b. The  $2F_o-F_c$  electron density map is contoured at 1.0 $\sigma$  and is displayed as a grey mesh.

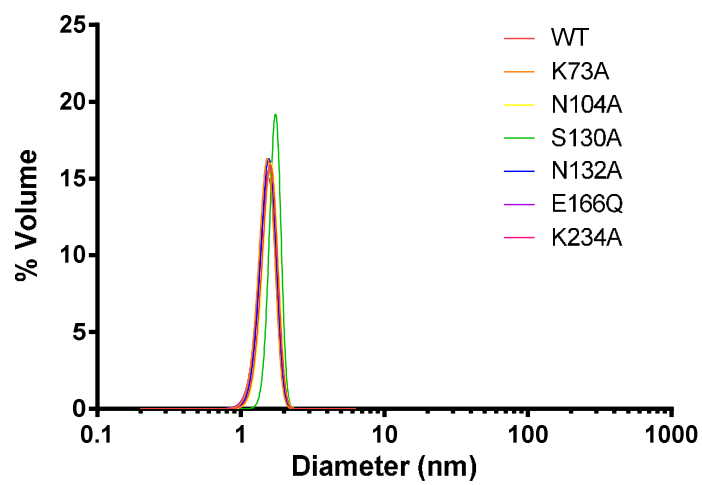


Figure S3. **CTX-M-15 variants are stable in solution.** Characterization of the particle size distribution for CTX-M-15 variants using dynamic light scattering.



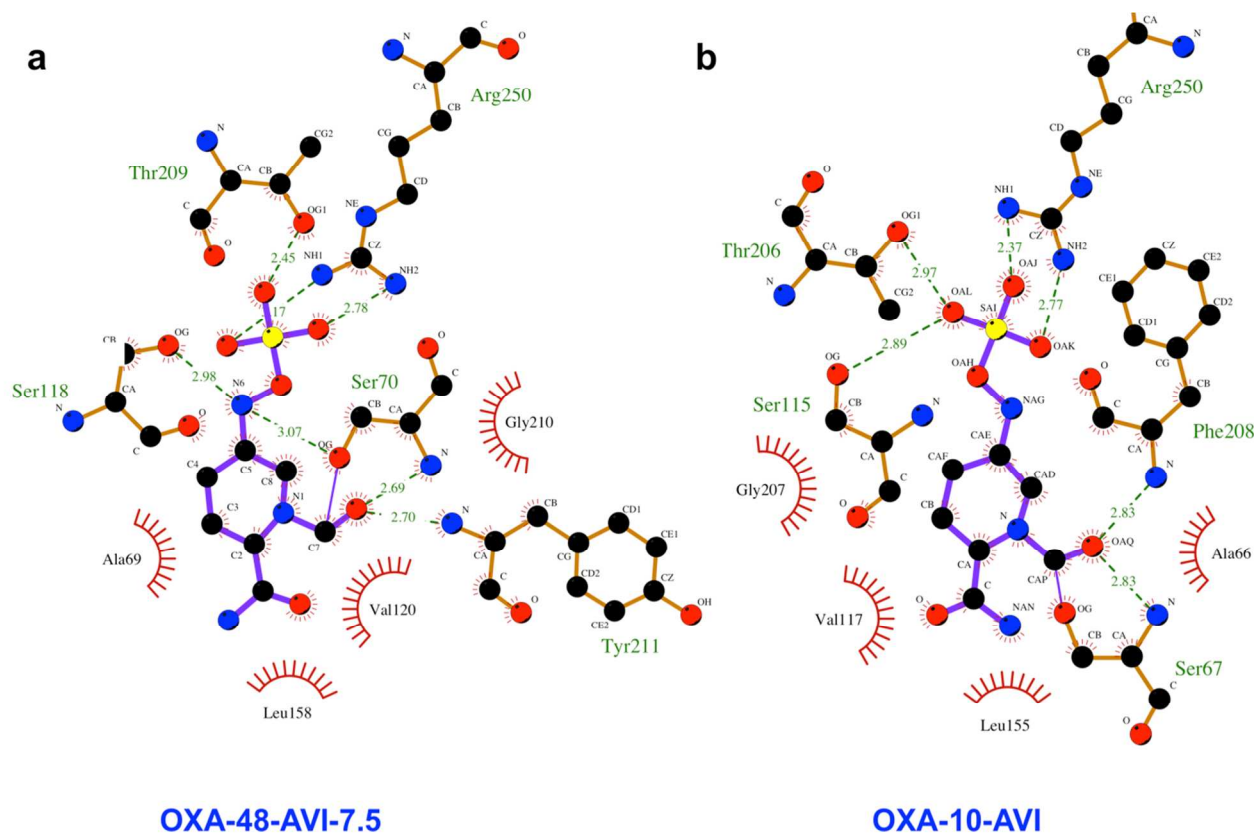


Figure S4. Interactions between avibactam and active site residues in OXA-48 and OXA-10. (a) and (b), Chain A-avibactam interactions in OXA-48-AVI-7.5 and OXA-10-AVI crystal complexes designed using LigPlot<sup>+</sup> <sup>3</sup>. In all panels, the carbamyl-avibactam and active site residues are displayed as purple and orange sticks with atoms colored by type. Hydrogen bonding and electrostatic interactions are shown as green dashes. Ligand-protein hydrophobic contacts are displayed as curved red combs.

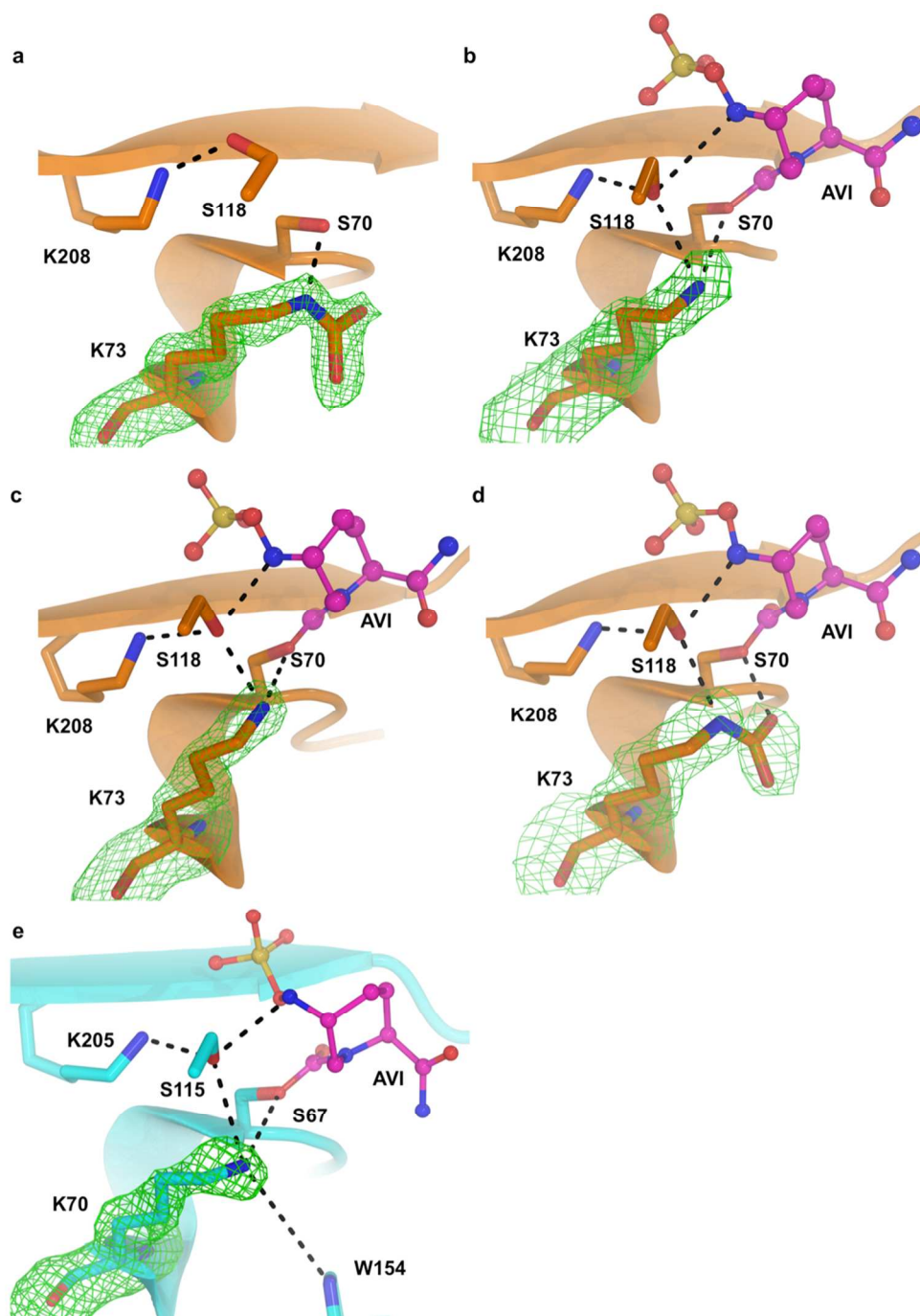


Figure S5. Carboxylation state of the SXXK lysine in OXA-48 and OXA-10. (a) Native OXA-48 (pH 7.5), chain A K73 omit  $F_o - F_c$  electron density. The OXA-48 protein backbone is displayed as an orange cartoon with selected active site residues shown as sticks with all non-carbon atoms colored by type. The  $F_o - F_c$  K73 omit electron density map is contoured at  $3.0\sigma$  and is shown as a green mesh. (b), (c) and (d) OXA-48-AVI6.5 (pH 6.5), OXA-48-AVI7.5 (pH 7.5) and OXA-48-AVI8.5 (pH 8.5), chain A K73 omit  $F_o - F_c$  electron density. The OXA-48 protein backbone, active site residues and  $F_o - F_c$  K73 omit electron density maps are shown as in A. The carbamyl-avibactam is represented as pink sticks with all non-carbon atoms colored by type. (e) OXA-10-AVI (pH 6.5) chain A K70 omit  $F_o - F_c$  electron density map. The OXA-10 protein backbone is displayed in cyan cartoon representation with selected active site residues shown as sticks with all non-carbon atoms colored by type. The  $F_o - F_c$  K70 omit electron density map is represented as in a. The carbamyl-avibactam is represented as in b.

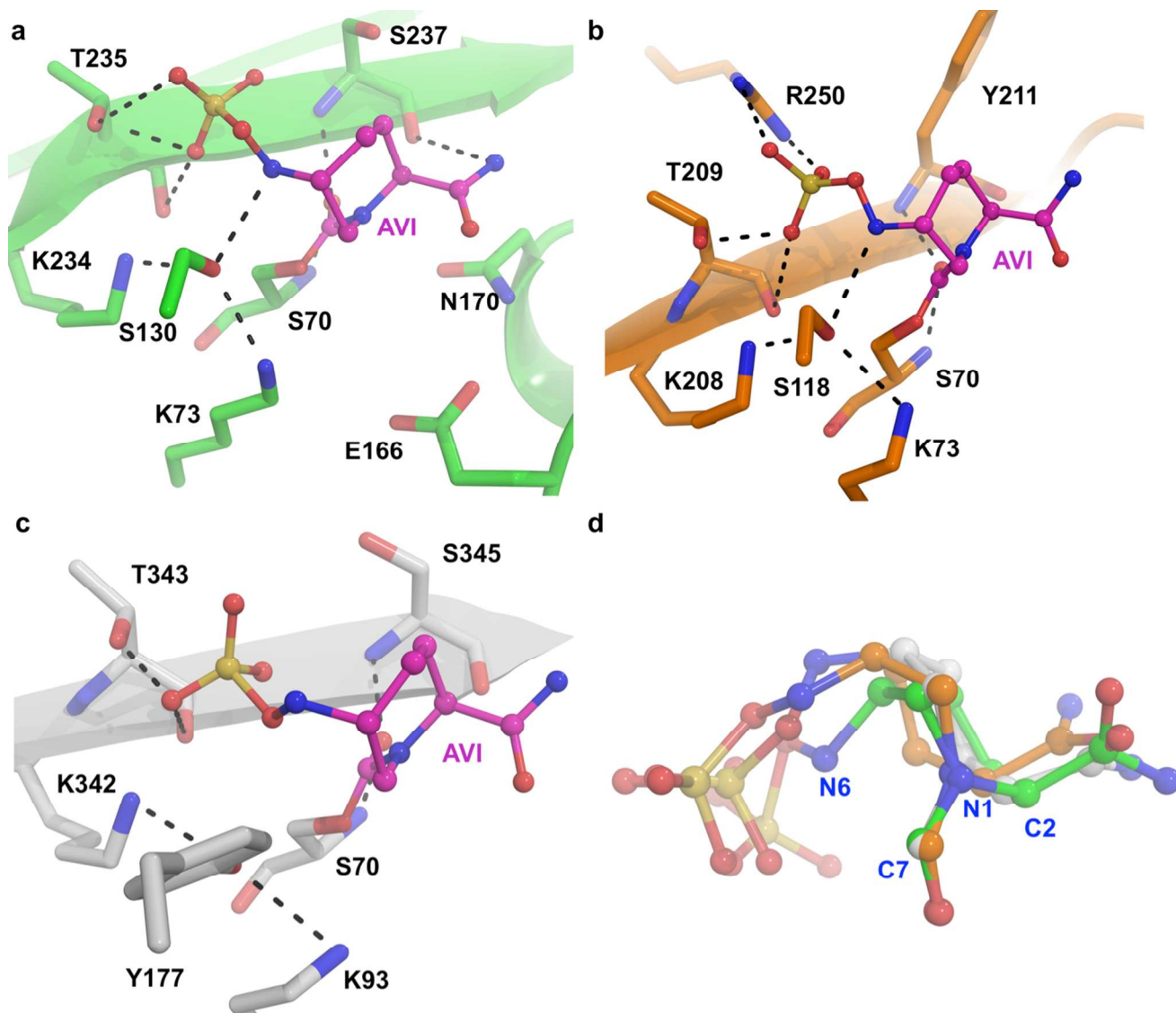

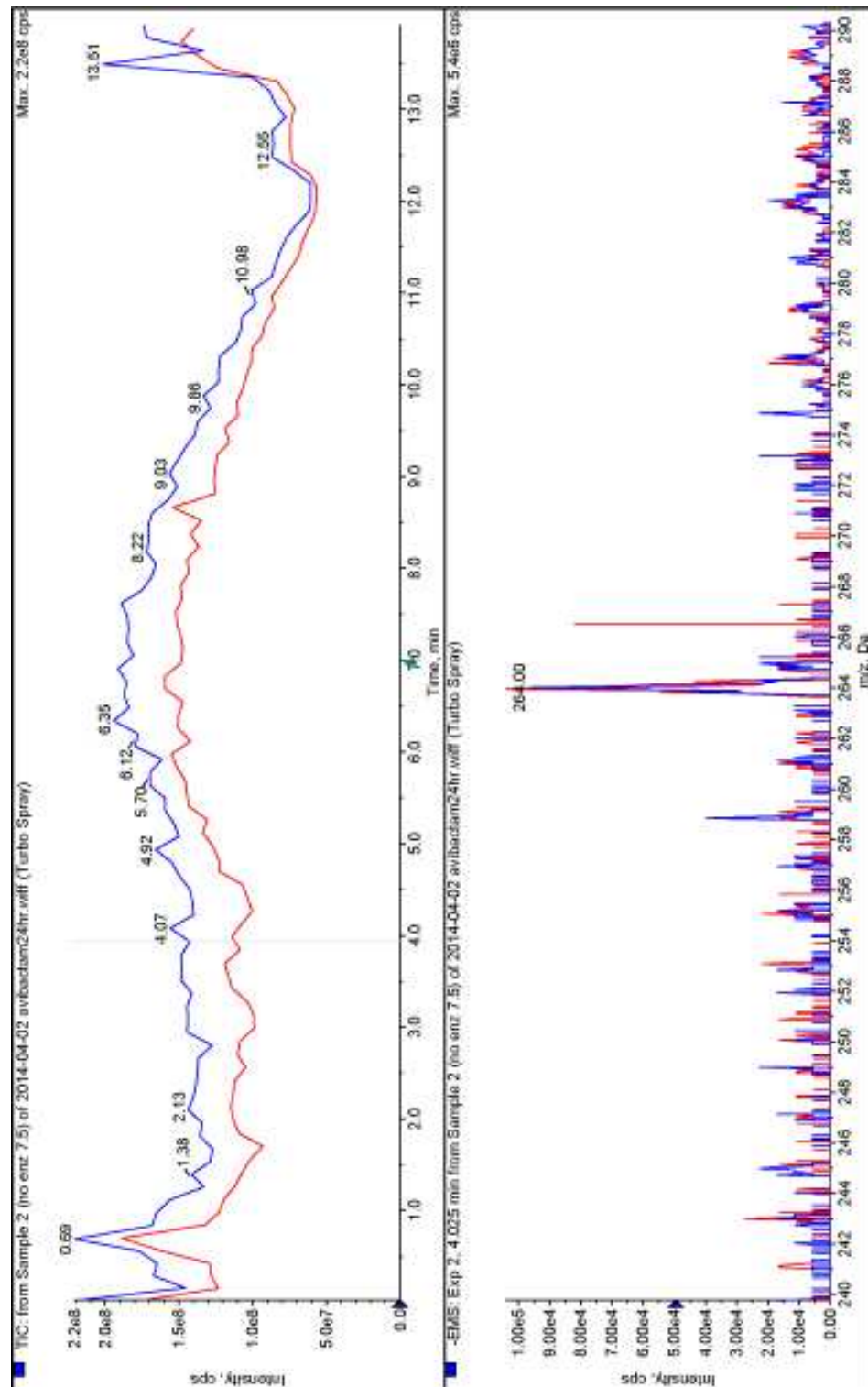
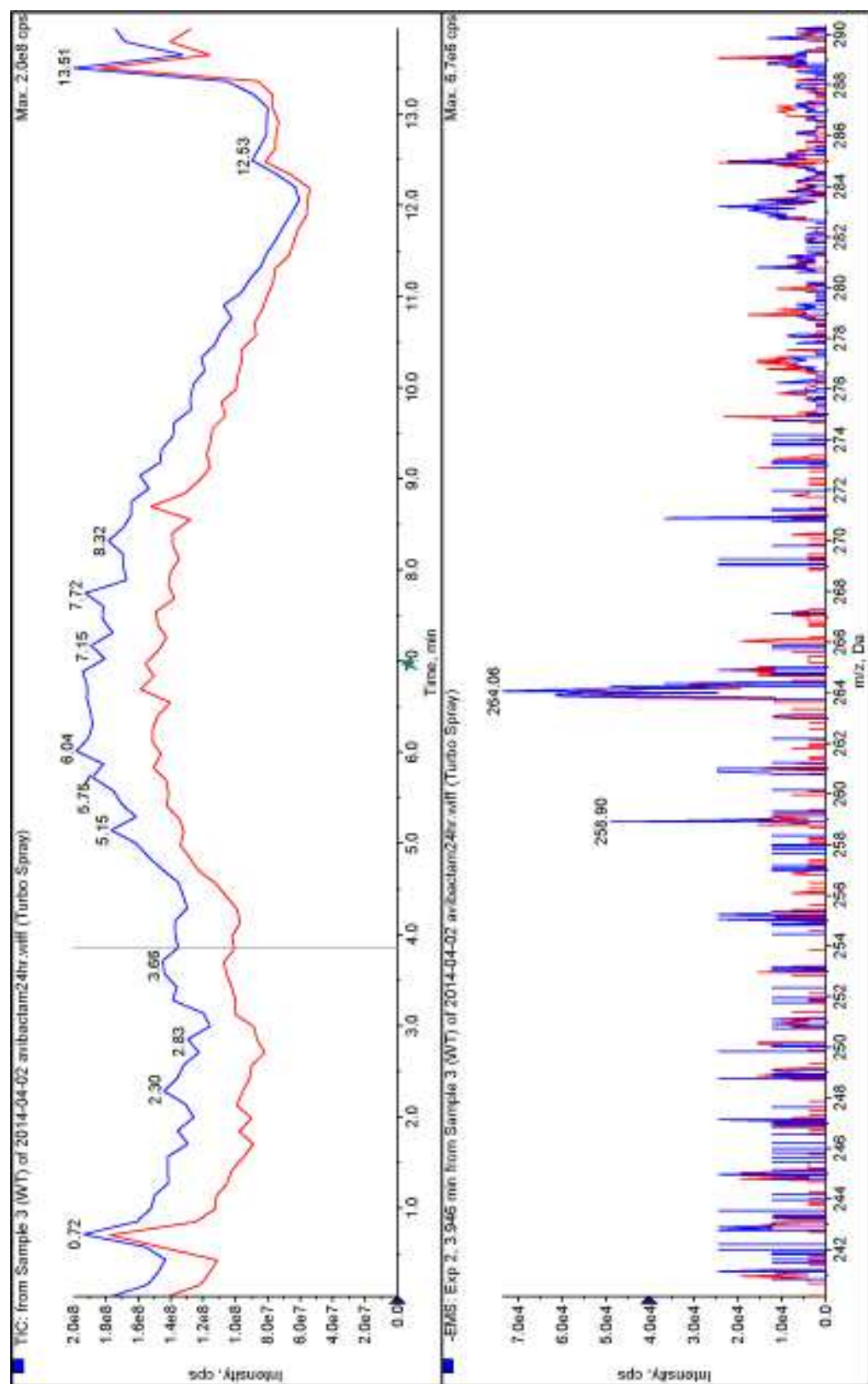


Figure S6. Comparison of carbamyl-avibactam CTX-M-15, OXA-48 and AmpC co-crystal structures. (a) Active site close-up of carbamyl-avibactam CTX-M-15. The carbon atoms of avibactam are pink with non-carbon atoms colored by atom type. The avibactam bound CTX-M-15 protein chain is represented as a green cartoon, with key active site residues shown as sticks with atoms colored by type. (b) and (c) Active site overlay of carbamyl-avibactam OXA-48, and AmpC (PDB ID: 4HEF)<sup>2</sup>. In b and c, the bound avibactam is represented as in a. The OXA-48 and AmpC protein chains are illustrated as orange and grey cartoons, and active site residues are depicted as sticks with non-carbon atoms colored by type. In a-c, hydrogen bonding and electrostatic interactions are shown as black dashes. (d) Overlay of carbamyl-avibactam from the CTX-M-15, OXA-48 and AmpC co-crystal structures (PDB ID's: XXXX, XXXX, 4HEF)<sup>2</sup>. Carbamyl-avibactam from the CTX-M-15, OXA-48 and AmpC structures are displayed as green, orange and white sticks with all non-carbon atoms colored by type. The carbamyl-avibactam C7 carbon, carbonyl oxygen and N1 atoms were fixed in the exact same positions.

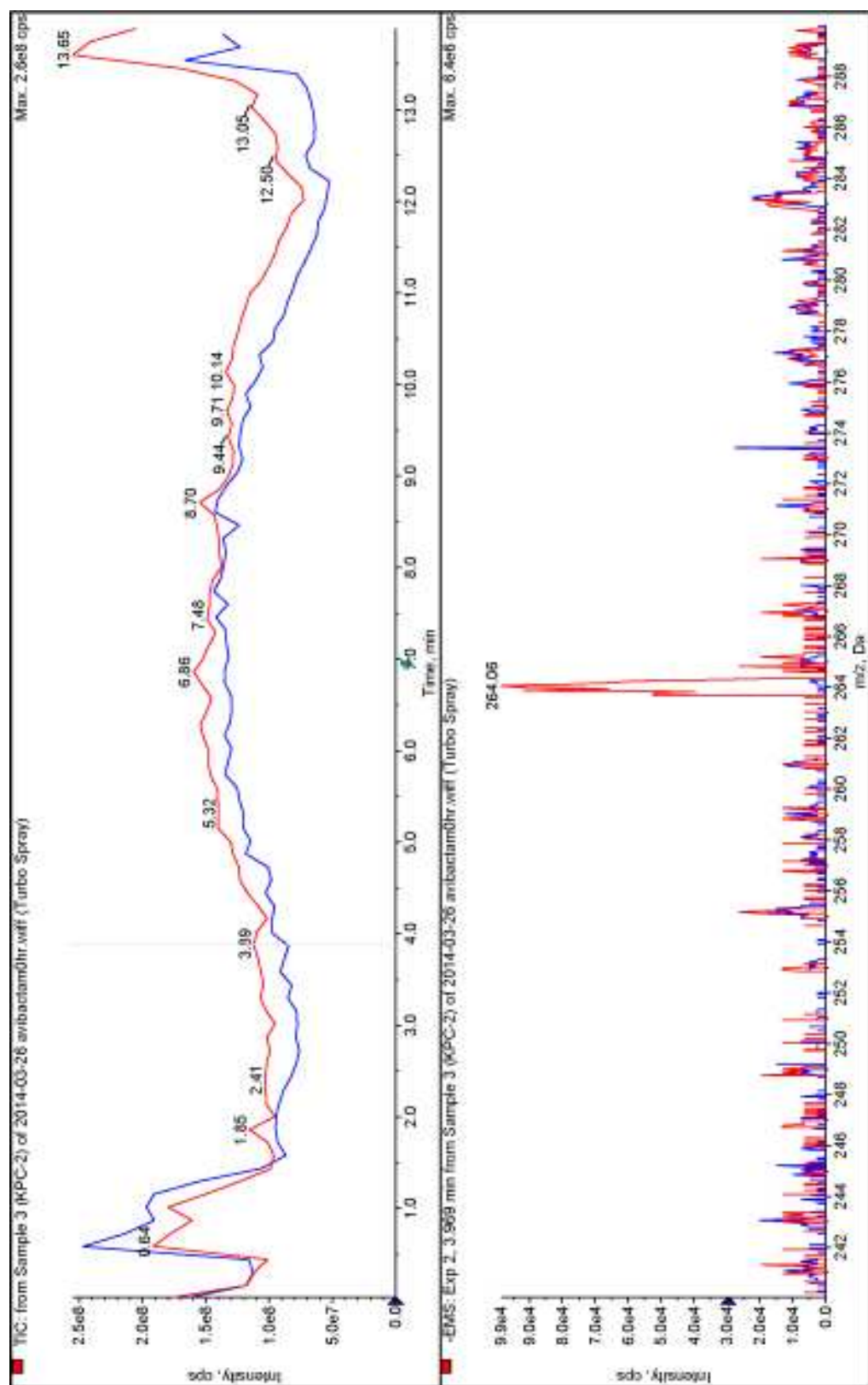
Figures S7-S16. ESI-LC-MS trace overlays of avibactam incubated with  $\beta$ -lactamase as noted at pH 7.5 (Figs S7-S15). Samples were analyzed at 0 hours (red trace) and 2 hours (blue trace). Avibactam remains intact in all samples with the exception of KPC-2 and no enzyme pH 8.5 

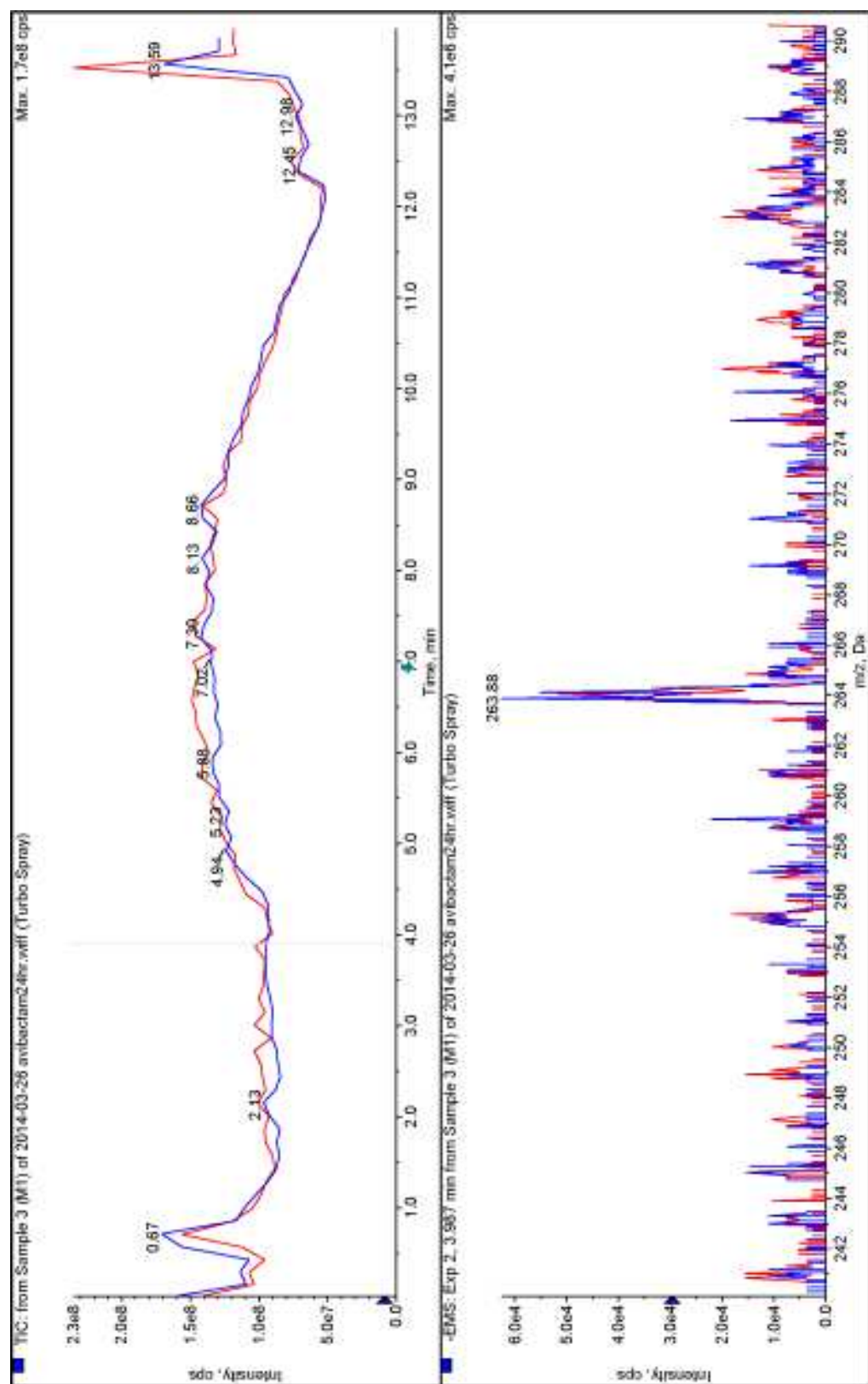
### No enzyme

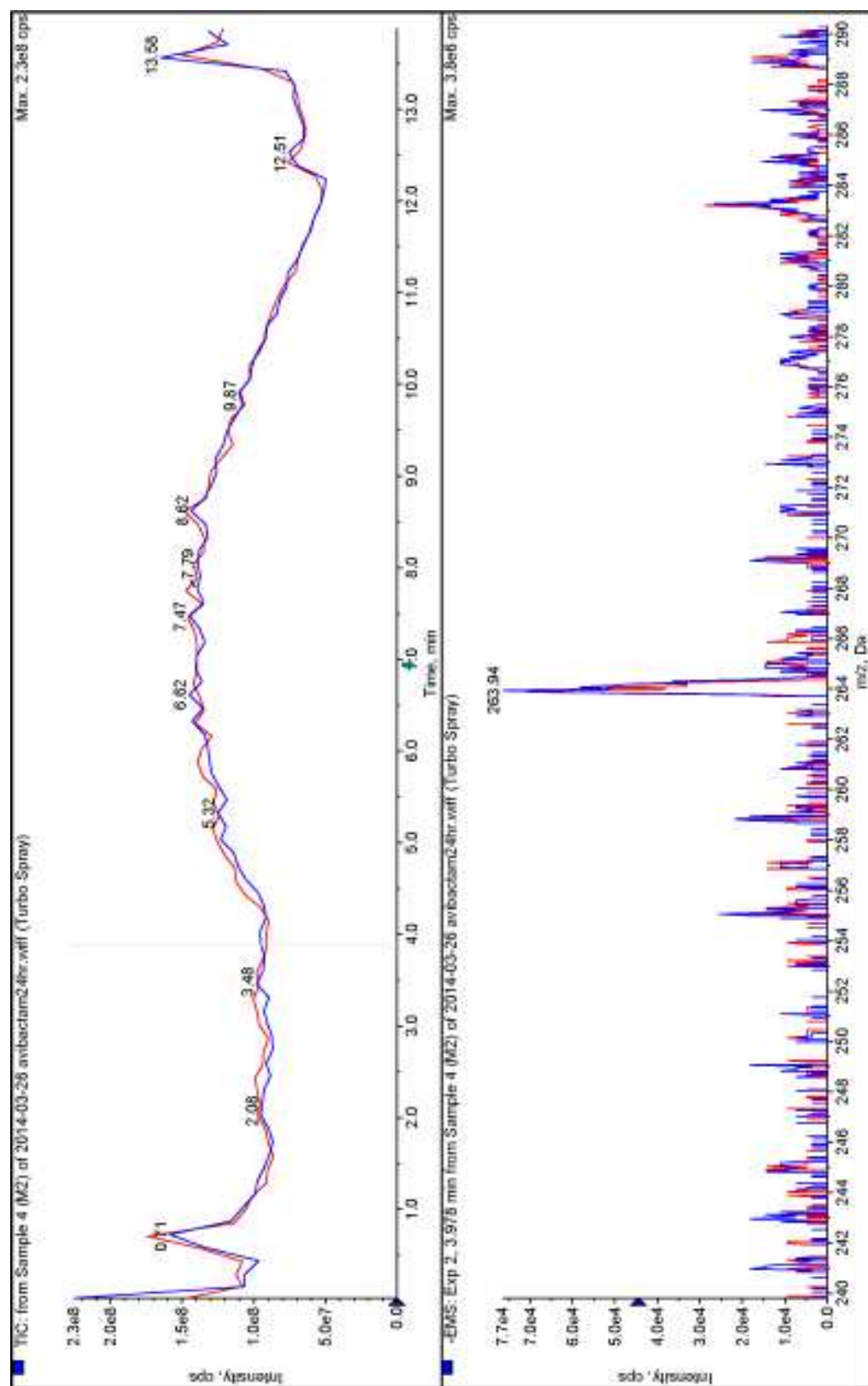




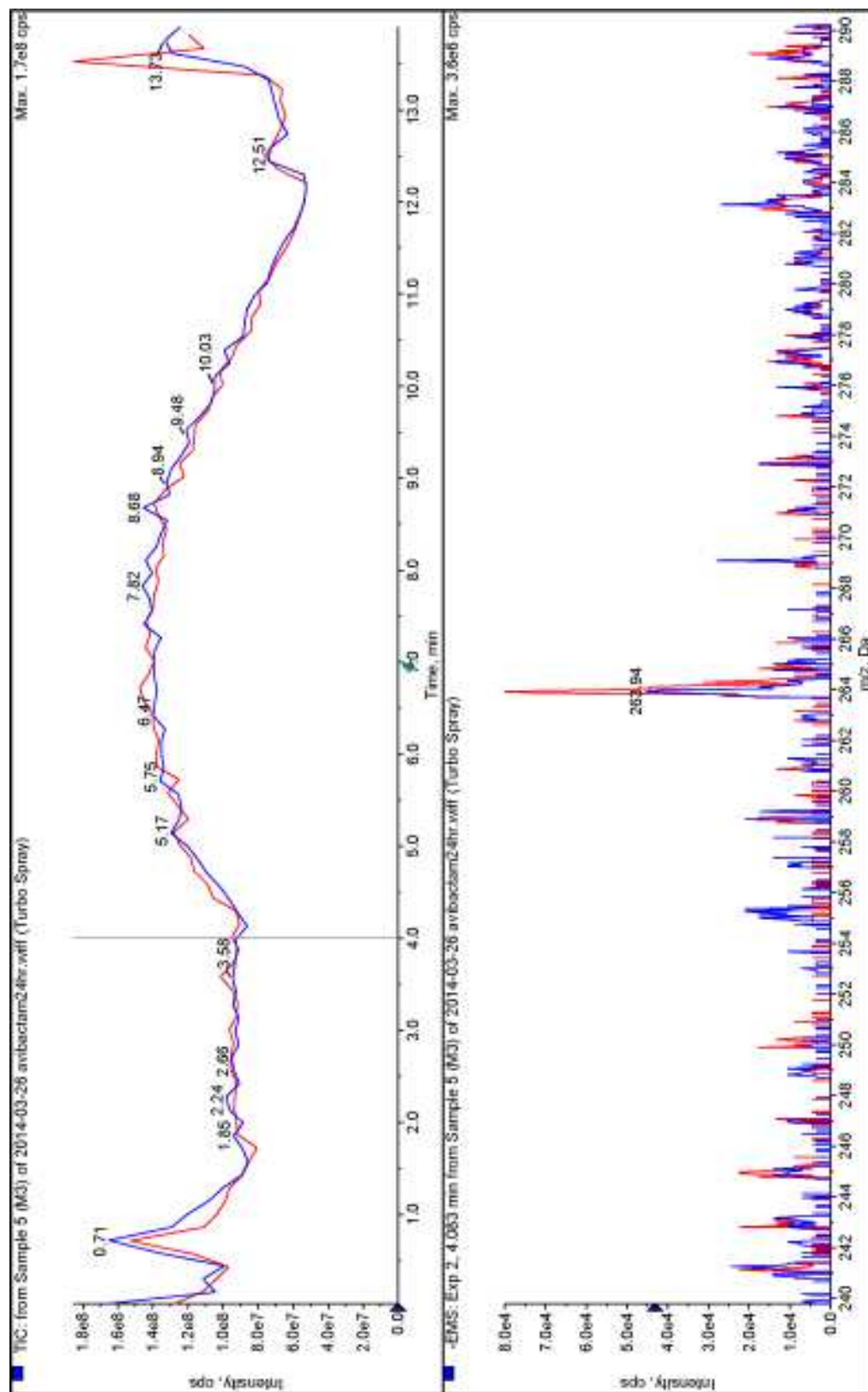


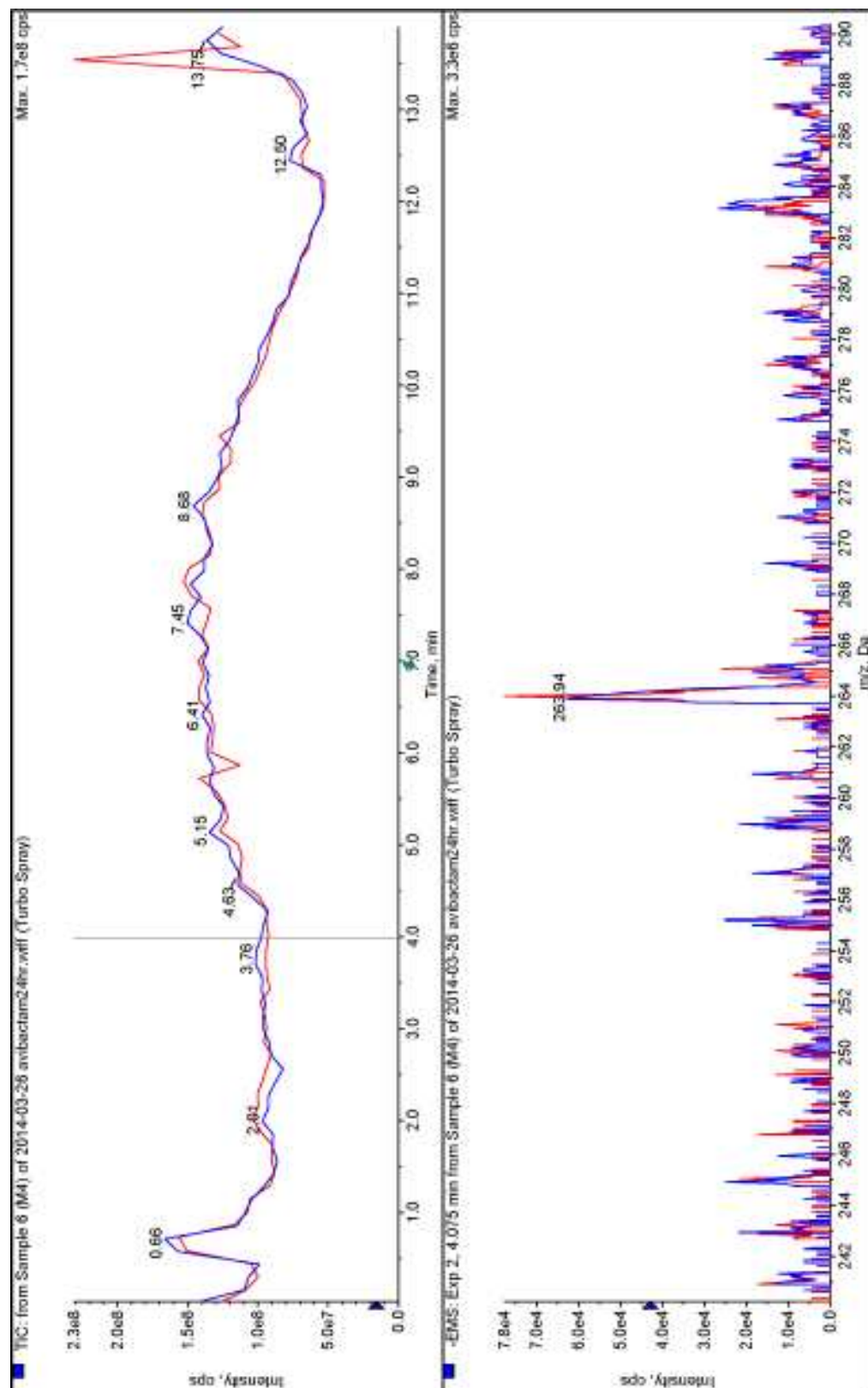


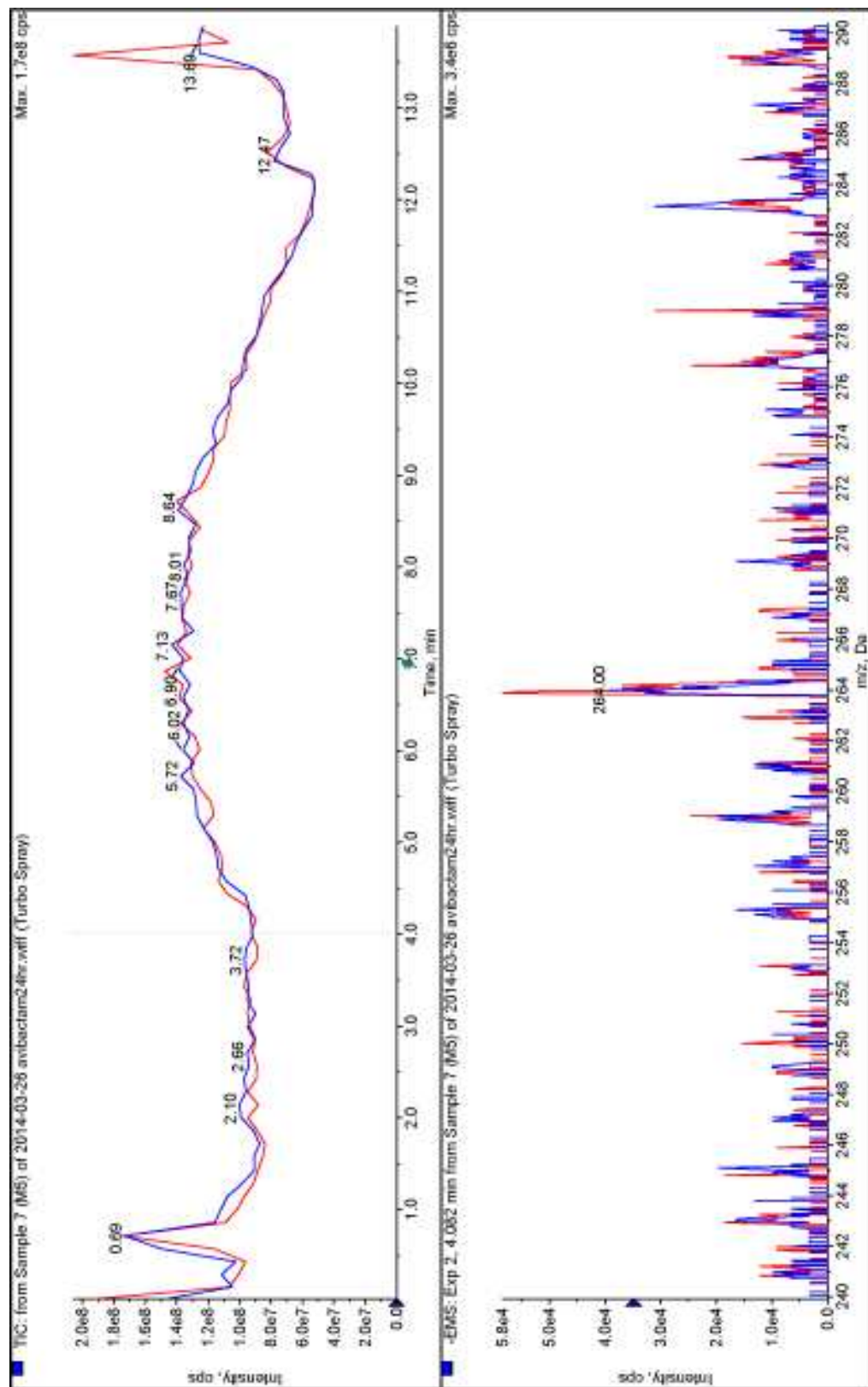


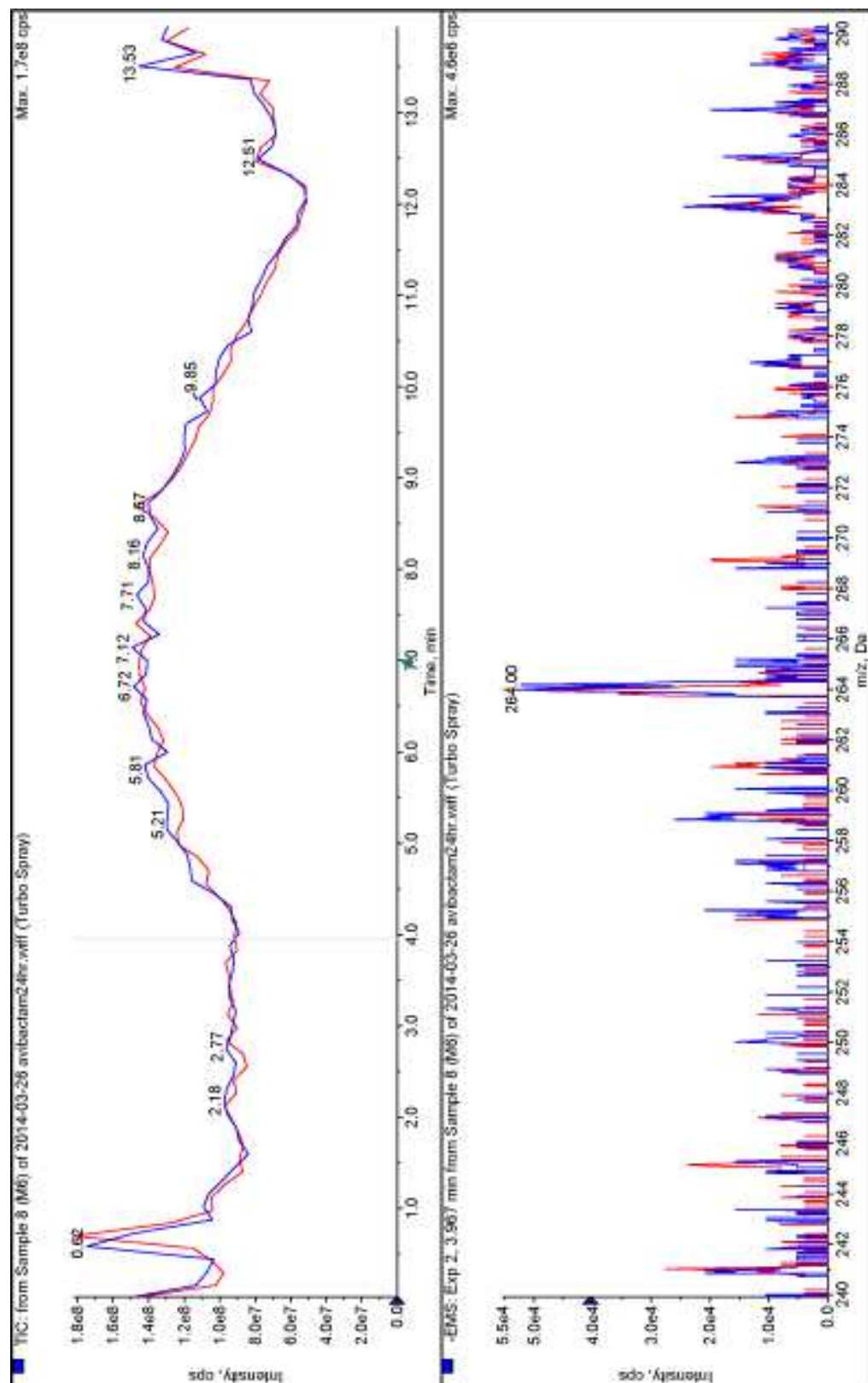




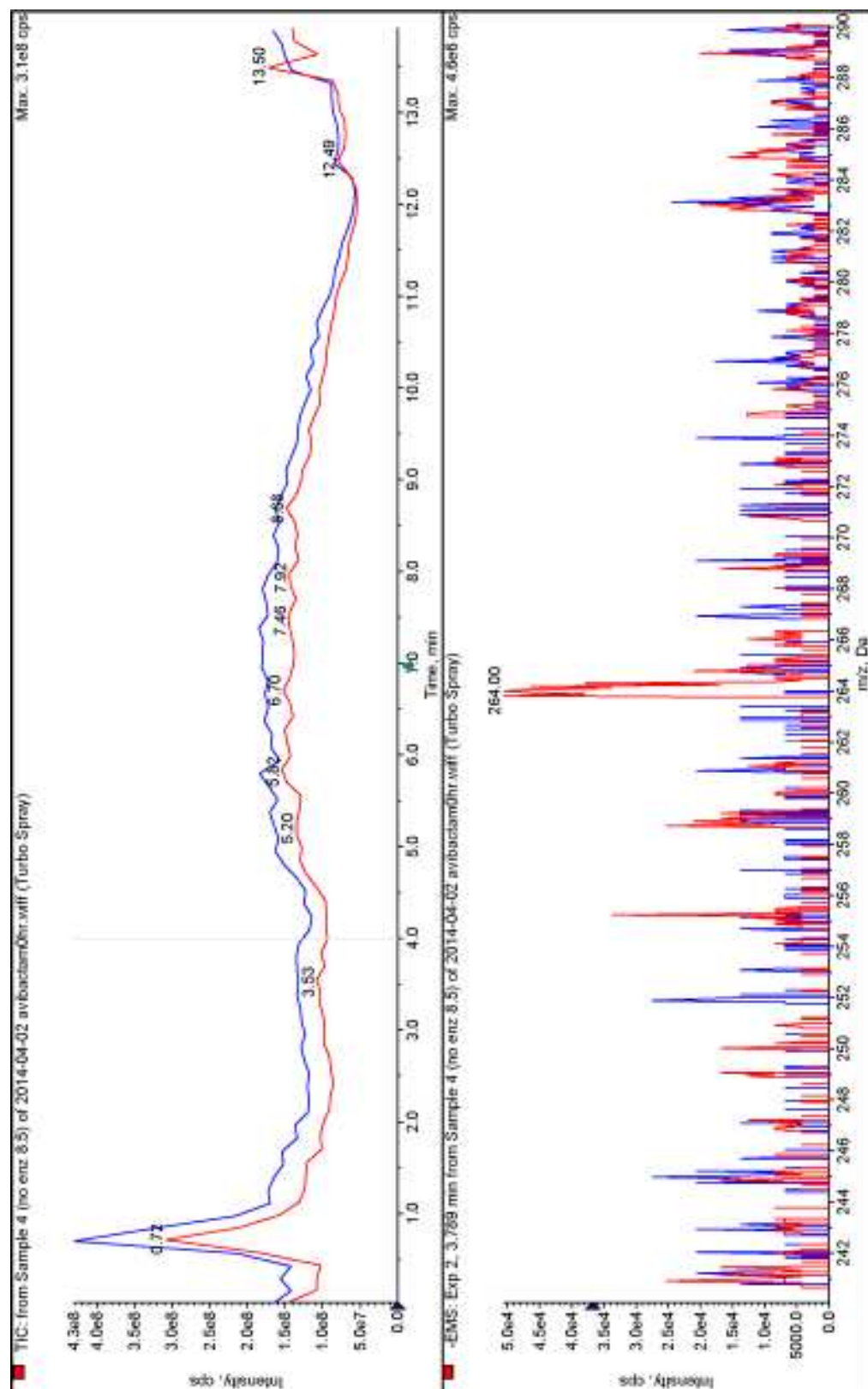








# No enzyme (pH 8.5)



## REFERENCES

1. Paetzel, M.; Danel, F.; de Castro, L.; Mosimann, S. C.; Page, M. G.; Strynadka, N. C., Crystal structure of the class D beta-lactamase OXA-10. *Nat Struct Biol* **2000**, *7* (10), 918-25.
2. Lahiri, S. D.; Mangani, S.; Durand-Reville, T.; Benvenuti, M.; De Luca, F.; Sanyal, G.; Docquier, J. D., Structural insight into potent broad-spectrum inhibition with reversible recyclization mechanism: avibactam in complex with CTX-M-15 and *Pseudomonas aeruginosa* AmpC  $\beta$ -lactamases. *Antimicrob Agents Chemother* **2013**, *57* (6), 2496-505.
3. Laskowski, R. A.; Swindells, M. B., LigPlot+: multiple ligand-protein interaction diagrams for drug discovery. *J Chem Inf Model* **2011**, *51* (10), 2778-86.